Probe-EM: Targeted Neuron Tracing via Training-Free Semantic Verification

Liuyun Jiang[1,2*], Yanchao Zhang[1,2*], Jinyue Guo[1,3], Chuanyue Chen[1,4], Haiyang Yan[1,2], Ye Yuan[1,4], Jing Liu[1(✉)], and Hua Han[1,2(✉)]

[1] State Key Laboratory of Brain Cognition and Brain-inspired Intelligence Technology, Institute of Automation, Chinese Academy of Sciences, Beijing, China
liujing2016@ia.ac.cn, hua.han@ia.ac.cn
[2] School of Future Technology, University of Chinese Academy of Sciences
[3] School of Artificial Intelligence, University of Chinese Academy of Sciences
[4] School of Advanced Interdisciplinary Sciences, University of Chinese Academy of Sciences

Abstract. Establishing large-scale, high-resolution neural connectivity maps is fundamental to elucidating the structural basis of brain function. However, when processing terabyte- or petabyte-scale electron microscopy data, over-segmentation inherent in automated reconstruction algorithms remains a critical bottleneck, requiring extensive manual proofreading spanning person-years. To alleviate the heavy reliance on annotated data and the limited flexibility of conventional tracing methods, we propose a training-free, targeted neuron tracing framework. Specifically, we introduce a skeleton-guided Heuristic Spatial Search paradigm that leverages geometric priors to iteratively reconstruct neuronal morphologies through a probing–verification cycle. To achieve robust zero-shot semantic verification, we further develop a Dimension-Aware Semantic Verification strategy built upon the foundation model NeuroSAM 2. This strategy resolves intra-slice splits via Planar Ensemble Consensus and inter-slice splits via Axial Spatio-Temporal Propagation. Notably, we integrate the proposed workflow into the Neuroglancer visualization platform, enabling an interactive human-in-the-loop proofreading system. Experimental results demonstrate that the proposed method outperforms supervised baselines and reduces manual proofreading time by 33.4%. The source code is publicly available at `https://github.com/HeadLiuYun/Probe-EM`.

Keywords: Connectomics · Neuron Segmentation · Volume Electron Microscopy · Deep Learning · Foundation Model.

1 Introduction

Connectomics aims to elucidate the structural foundations of brain function by reconstructing high-fidelity neural connectivity maps at nanometer resolution [6,13,21]. Driven by recent breakthroughs in electron microscopy (EM)

[*] These authors contributed equally.

imaging, connectomic datasets have rapidly expanded from localized circuits to whole-brain volumes at the terabyte-to-petabyte scale [1,17,19]. Nevertheless, current automated reconstruction methods [5,8,9,10,20] remain prone to over-segmentation errors, necessitating prohibitively labor-intensive manual proofreading to recover complete neuronal morphologies and connectivity. Given that proofreading a single *Drosophila* brain requires tens of person-years of human effort [4,16], developing efficient automated validation methods has become imperative to address scalability bottlenecks in modern connectomics [3].

To alleviate the substantial manual effort required for proofreading, a range of automated validation strategies has been developed to address over-segmentation in neuronal reconstructions. Existing frameworks primarily employ deep learning models to infer connectivity probabilities between neurite segments. For instance, Matejek et al. [12] utilized 3D CNNs on biologically constrained graphs to predict segment merges, while Chen et al. [2] leveraged multimodal contrastive learning to train high-performance classifiers. Similarly, RoboEM [18] introduced a self-steering system simulating flight navigation to connect segments in 3D space. Despite these advances, existing methods are hindered by two critical limitations. **(1) Rigid validation paradigm.** Most existing frameworks model error correction as a binary inference task between discrete segments. This approach necessitates exhaustive global scanning, which lacks the necessary flexibility for targeted neurite tracing. In practical scenarios where researchers prioritize specific neuronal populations, existing methods cannot initiate tracing directly from user-defined seed segments to reconstruct complete morphologies, resulting in substantial computational resources and time being unnecessarily consumed on non-target regions. **(2) Heavy reliance on annotated data.** Existing models depend heavily on large-scale ground-truth labels for supervised training, limiting their out-of-the-box generalizability when applied to novel datasets with distinct characteristics.

We propose a training-free, targeted neuron tracing framework to address these challenges. Specifically, the framework implements a Heuristic Spatial Search (HSS) paradigm that emulates human expert decision-making logic. This paradigm leverages skeleton-based geometric priors to autonomously explore and validate fragments within the spatial vicinity of a seed segment, thereby enabling efficient local-to-global topological reconstruction. This strategy avoids the computational redundancy inherent in conventional global scanning approaches for non-target regions. To reduce the dependency on large-scale annotations required by existing supervised methods, we develop a Dimension-Aware Semantic Verification (DASV) module, anchored by **NeuroSAM 2**, a foundation model [15] specifically fine-tuned for neuronal EM imagery. To ensure robust connectivity inference, the DASV module handles intra-slice and inter-slice split scenarios using a Planar Ensemble Consensus (PEC) and an Axial Spatio-Temporal Propagation (ASP) mechanism, respectively. Finally, we integrate the proposed algorithm into the Neuroglancer [5] visualization platform to construct a human-in-the-loop interactive proofreading system.

[5] https://github.com/google/neuroglancer

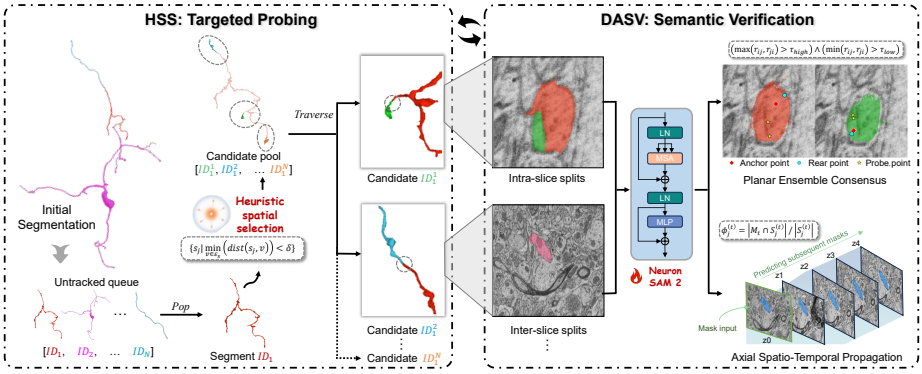

Fig. 1. Overview of Probe-EM. The framework facilitates iterative tracing of complete neuronal morphologies through a synergistic probing-verification cycle.

The primary contributions of this work are summarized as follows: (1) We propose the HSS tracing paradigm, which leverages skeleton geometric priors to guide targeted neurite growth, thereby eliminating the computational redundancy inherent in conventional global scanning approaches. (2) We introduce NeuroSAM 2 and the DASV strategy to achieve training-free automated validation across both intra-slice and inter-slice split scenarios. (3) Experiments on the SCN dataset demonstrate that our framework outperforms supervised baselines, reducing manual proofreading time by 33.4% while maintaining high reconstruction fidelity.

2 Method

As illustrated in Fig. 1, this work introduces a seed-guided active tracing paradigm that circumvents the computational redundancy inherent in conventional global approaches within non-target regions. The proposed framework incorporates an HSS module for targeted candidate probing alongside a DASV module for multi-dimensional connectivity inference. By leveraging the iterative refinement of a probing-verification cycle, our approach achieves efficient, high-fidelity reconstruction of neuronal topology.

2.1 HSS: Targeted Probing

We reformulate the neuron tracing problem as a targeted, seed-driven retrieval task. Let $\mathcal{V}$ denote the set of all segments within a volume, and let a complete biological neuron N be represented by a subset of segments $\mathcal{S}_N \subseteq \mathcal{V}$, defined as $\mathcal{S}_N = \{s_1^{(N)}, s_2^{(N)}, \ldots, s_n^{(N)}\}$. Given a specific seed segment $s_{seed} \in \mathcal{S}_N$, the goal is to efficiently recover the remaining components $\mathcal{S}_N \setminus \{s_{seed}\}$ through iterative local exploration. Unlike conventional methods that rely on exhaustive pairwise connectivity predictions across the entire volume $(s_i, s_j) \in \mathcal{V} \times \mathcal{V}$, our targeted

formulation naturally enables flexible, seed-driven tracing, prioritizing specific neuronal populations.

A processing queue Q is maintained, initialized with a seed segment s_{seed}. In each iteration, the algorithm dequeues a segment s and applies a skeletonization operator $\Gamma(s)$ to extract its spatial topology, represented as a graph $G_s = (V, E)$. Given that neuronal discontinuities predominantly occur at skeleton terminals, we explore adjacent fragments within spherical neighborhoods centered at each endpoint in the terminal set $\mathcal{E}_s = \{v \in V \mid \deg(v) = 1\}$. The candidate set $\mathcal{C}$ for the subsequent DASV module is formally defined as:

$$\mathcal{C} = \{s_j \in \mathcal{V} \mid \min_{v \in \mathcal{E}_s} \|\text{pos}(s_j) - \text{pos}(v)\|_2 < \delta\} \tag{1}$$

where $\text{pos}(\cdot)$ denotes 3D coordinates and $\delta = 500\,\text{nm}$ is the search radius, ensuring sufficient coverage for potential continuities.

To mitigate error propagation and prevent computational divergence, a topological pruning mechanism is incorporated into the HSS module. During the tracing cycle, the algorithm continuously monitors the topological complexity of the growth front. When a newly detected segment exhibits an excessive number of endpoints or abnormal skeleton endpoint density—morphological signatures typically associated with glial cell misconnections or reconstruction mergers—it is identified as a topological anomaly, and the expansion of that branch is preemptively terminated. Segments that pass this topological validation are subsequently integrated into the global topology and appended to the queue Q for further exploration. This procedure iterates until Q is empty, thereby achieving a comprehensive reconstruction of the neuronal topological morphology.

2.2 DASV: Semantic Verification

The DASV module evaluates the candidate set $\mathcal{C}$ generated by HSS, leveraging multi-dimensional semantic features to verify inter-segment connectivity. Candidate pairs are categorized into two distinct scenarios: **intra-slice splits** occurring within the same XY plane, and **inter-slice splits** spanning multiple Z-axis slices. This dimension-aware classification enables specialized verification strategies tailored to the specific reconstruction challenges inherent in each scenario.

Planar Ensemble Consensus. In intra-slice scenarios, the principal challenge lies in discerning genuine semantic boundaries between candidate segments. To address this, we leverage NeuroSAM 2, a foundation model fine-tuned on neuronal EM datasets, to perform connectivity verification via a bi-directional ensemble consensus task.

Specifically, the procedure begins with a robust geometric prompt sampling strategy. For a candidate pair (s_i, s_j), Euclidean distance transforms are utilized to extract three types of complementary prompt points shown in Fig. 1: (1) anchor points at morphological centers to establish segment identity; (2) probe points positioned in close proximity to the target segment to test boundary permeability; and (3) rear points located distal to the target to ensure that NeuroSAM 2 maintains the morphological integrity of the segment during mask

expansion. During the verification stage, the algorithm executes $K = 5$ independent randomized trials. Each trial performs a cross-prediction: predicting s_j given prompts from s_i, and vice versa, to calculate the bidirectional overlap ratios r_{ij} and r_{ji}. A trial is considered successful only if the scores satisfy a dual-threshold criterion:

$$(\max(r_{ij}, r_{ji}) > \tau_{\text{high}}) \wedge (\min(r_{ij}, r_{ji}) > \tau_{\text{low}}) \tag{2}$$

where τ_{high} and τ_{low} enforce both strong merging evidence and minimal bidirectional agreement. Final connectivity is confirmed only when an ensemble consensus is achieved (e.g., passing 4 out of 5 trials). This stringent voting logic leverages the boundary awareness of NeuroSAM 2 while effectively suppressing false connections resulting from mask leakage or sampling stochasticity.

Axial Spatio-Temporal Propagation. Verifying inter-slice axial splits poses significant challenges, as these discontinuities frequently span multi-slice Z-axis gaps. Conventional methods typically rely on Intersection over Union (IoU) matching between adjacent slice masks. However, such heuristics are highly susceptible to slice misalignments, tissue loss, or drastic morphological shifts of neurites, thereby failing to maintain long-range topological robustness. To address these limitations, we leverage the long-range modeling capabilities of NeuroSAM 2 to introduce an axial spatio-temporal propagation mechanism.

Specifically, the algorithm formulates the 3D neighborhood of a split as a pseudo-video sequence aligned along the Z-axis. Using the mask of the source segment as the initial prompt, the convolutional memory module within NeuroSAM 2 is driven to autonomously propagate and evolve the segment identity along the axial direction for N frames. In contrast to static IoU matching, this memory-augmented propagation effectively captures and adapts to the morphological evolution of neurites across consecutive slices. During the N-frame mask evolution powered by NeuroSAM 2, the algorithm dynamically monitors the spatial overlap between the prediction and potential candidates through volumetric occupancy detection.

Formally, let M_t and $S_j^{(t)}$ denote the predicted mask and the voxel set of candidate segment s_j at frame t, respectively. The instantaneous connectivity score is computed as $\phi_j^{(t)} = |M_t \cap S_j^{(t)}|/|S_j^{(t)}|$. To identify the most robust connection throughout the traversal, the maximum coverage ratio across the propagation sequence is extracted as the final score: $\Phi_j = \max_{t\in\{1,\dots,N\}} \phi_j^{(t)}$. Long-range topological continuity is confirmed if Φ_j exceeds a predefined semantic collision threshold τ_{occ}.

Finally, the HSS and DASV modules are integrated into the Neuroglancer visualization platform, creating an interactive, human-in-the-loop proofreading system.

3 Experiments

3.1 Datasets and Evaluation Metrics

We utilized the first complete serial section electron microscopy (ssEM) dataset of a unilateral mouse suprachiasmatic nucleus (SCN) [11]. With a voxel resolution of $5 \times 5 \times 40$ nm^3, the dataset comprises 6,824 serial sections and covers a physical volume of approximately 0.06 mm^3, amounting to a raw data size of 88.3 TB. The SCN dataset was processed using a 3D Residual U-Net [10] to generate affinity maps, followed by the distance transform watershed algorithm [7] to obtain the initial segmentation results. The SCN dataset is characterized by prominent cable-like axon fascicles traversing the nucleus. However, these slender and elongated structures are inherently susceptible to over-segmentation errors during automated 3D reconstruction. We annotated a total of 36 axon fascicles and 12 soma-containing neurons. Of these, 12 axon fascicles and 4 soma-containing neurons were selected to train the learning-based baseline methods [2,12], while the remainder constituted the test set.

To quantitatively evaluate the tracing framework, we adopt a skeleton-node-based evaluation metric. Specifically, Recall, Precision, and F1 scores are computed by comparing the skeleton nodes covered by the retrieved segments against the ground-truth nodes. Crucially, nodes belonging to the initial seed segment are excluded from all metric calculations to strictly assess the algorithm's incremental tracing efficacy.

3.2 Implementation Details

We implemented learning-based baselines [2,12,14] for comparison. The baselines were trained on $120 \times 120 \times 30$ volumetric patches centered at potential junctions. Models were optimized for 50 epochs using binary cross-entropy loss and the Adam optimizer (lr$=1 \times 10^{-4}$), employing a `WeightedRandomSampler` for class imbalance (433 positive/8,699 negative pairs). Unlike these supervised models, our framework performs training-free connectivity inference. Although NeuroSAM 2 adapts SAM 2 by fine-tuning the prompt encoder and mask decoder (keeping the image encoder frozen) on EMNeuron [22] for general EM features, it strictly excludes connectivity supervision, enabling zero-shot semantic verification. For DASV, we set $\tau_{\text{high}} = 0.5$, $\tau_{\text{low}} = 0.1$, $\tau_{\text{occ}} = 0.6$, and window size $N = 5$. Experiments were conducted on a single NVIDIA RTX 4090 GPU.

3.3 Results

Neuron tracking performance. Experiments are categorized into two distinct tasks: **Axon Fascicle Tracing**, which aims to reconstruct the complete morphology starting from a localized seed segment within an axon bundle, and **Soma-seeded Tracing**, which focuses on the reconstruction of full neuronal structures originating from a soma-containing segment. For comparative evaluation, we benchmark our method against connectivity discrimination approaches

Table 1. Quantitative performance comparison of neuron tracing on the SCN dataset.

Methods	Axon Fascicle Tracing			Soma-seeded Tracing		
	Recall	Precision	F1	Recall	Precision	F1
Learning-based Methods						
Voxel-based CNN [12]	0.542	**0.902**	0.571	0.245	0.428	0.293
Geometric PointNet [14]	0.509	0.485	0.288	0.181	0.498	0.210
Multimodal Fusion [2]	0.421	0.650	0.436	0.160	0.372	0.202
Training-free Methods						
Ours (w/ SAM 2)	0.736	0.494	0.467	0.492	0.312	0.310
Ours (w/ NeuroSAM 2)	**0.753**	0.626	**0.595**	**0.705**	**0.565**	**0.544**

Table 2. Quantitative comparison of annotation efficiency and accuracy between manual-only and Probe-EM-assisted workflows.

Annotator	Manual Only		w/ Probe-EM		Improvement	
	Time (min)	F1 Score	Time (min)	F1 Score	Δ Time	Δ F1
Annotator 1	52.6	0.874	29.2	0.892	-44.5%	+2.1%
Annotator 2	31.6	0.827	20.0	0.974	-36.7%	+17.8%
Annotator 3	30.2	0.894	24.5	0.899	-18.9%	+0.6%
Average	**38.1**	**0.865**	**24.6**	**0.922**	**-33.4%**	**+6.8%**

based on voxel-wise morphological learning [12], point-cloud geometric learning [14], and a multimodal framework [2] that integrates both representations. Additionally, we evaluate the impact of the foundation model by contrasting the off-the-shelf SAM 2 [15] with our fine-tuned NeuroSAM 2 within the proposed framework. The quantitative results, summarized in Table 1, demonstrate that our method achieves the best overall performance, significantly outperforming the supervised learning-based baselines. We attribute this superiority to the inherent limitation of supervised approaches: they typically require extensive annotated pairs to capture the drastic morphological variations of segment cross-sections. In contrast, our approach leverages the robust generalization capabilities of the foundation model to handle such diversity effectively without heavy reliance on task-specific training data. These results are visually demonstrated in Fig. 2, where our method achieves superior topological integrity.

Human-in-the-loop Efficiency Study. To assess the practical impact of our framework on the proofreading workflow, we conducted a comparative user study involving three experienced annotators, each assigned to proofread five distinct neurons. As detailed in Table 2, the integration of Probe-EM significantly expedited the neurite proofreading process compared to the manual-only baseline. On average, the proofreading time was reduced from 38.1 to 24.6 minutes, yielding a 33.4% efficiency gain. Crucially, this acceleration was accompanied by a concurrent improvement in tracing quality, with the mean F1 score increasing by 6.8%. These results indicate that the suggestions provided by Probe-EM not only mitigate the manual annotation burden but also effectively assist annotators in

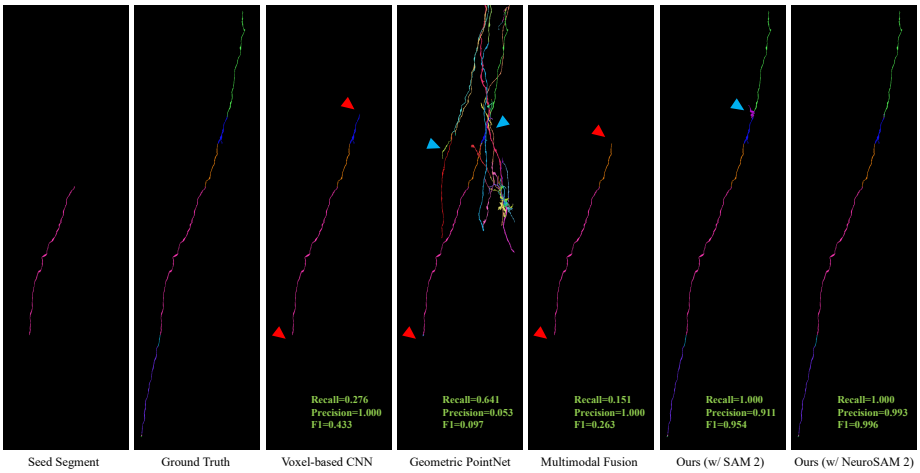

Fig. 2. Qualitative visualization of neuron tracing results. The leftmost Seed Segment serves as the input for comparison against the Ground Truth and various methods. Red and blue triangles highlight regions of incomplete tracing (missed neurites) and erroneous tracking (spurious fragments), respectively.

identifying branches that are frequently overlooked during manual slice-by-slice inspection.

Table 3. Ablation study of core components and hyperparameters. GPS denotes Geometric Prompt Sampling, and N represents the axial propagation window size.

Configuration	PEC	ASP	GPS	N	Recall	Precision	F1
w/o PEC		✓	✓	5	0.595	0.605	0.483
w/o ASP	✓		✓	5	0.020	**0.800**	0.036
w/o GPS	✓	✓		5	0.588	0.346	0.328
Ours ($N = 3$)	✓	✓	✓	3	0.611	0.624	0.484
Ours (Default)	✓	✓	✓	5	**0.691**	0.639	**0.586**
Ours ($N = 8$)	✓	✓	✓	8	0.589	0.396	0.371

Ablation Studies. To evaluate the efficacy of the core components within our framework, comprehensive ablation experiments were conducted on five distinct neurons from each task, as summarized in Table 3. These results demonstrate that both the ASP and PEC modules are indispensable. Notably, removing the ASP module leads to a precipitous drop in recall, indicating that most neurite discontinuities occur along the z-axis and underscoring the necessity of inter-slice propagation. Furthermore, the Geometric Prompt Sampling strategy significantly outperforms naive center-point prompting, as the strategic incorporation of probe and rear points better preserves the semantic integrity of the

segments. Finally, we evaluate the impact of the axial propagation window size N. A smaller window limits the capacity to bridge extensive spatial gaps, whereas an excessively large window accumulates propagation errors and introduces semantic drift, ultimately degrading precision.

4 Conclusion

We proposed Probe-EM, a training-free tracing framework. By combining HSS with NeuroSAM 2-based DASV, our method improves performance while reducing manual proofreading time by 33.4%, providing efficient support for complex neuron reconstruction and validation workflows in large-scale connectomics.

Acknowledgments. This work was supported by the Brain Science and Brain-like Intelligence Technology – National Science and Technology Major Project (2021ZD0204500, 2021ZD0204503), and the National Key Research and Development Program of China (2025YFA1614600).

Disclosure of Interests. The authors have no competing interests to declare that are relevant to the content of this article.

References

1. Functional connectomics spanning multiple areas of mouse visual cortex. Nature **640**(8058), 435–447 (2025)
2. Chen, Q., Chen, X., Wang, C., Liu, Y., Xiong, Z., Wu, F.: Learning multimodal volumetric features for large-scale neuron tracing. In: Proceedings of the AAAI Conference on Artificial Intelligence. vol. 38, pp. 1174–1182 (2024)
3. their Comment, I., Khajeh, R.: Method of the year 2025: electron microscopy-based connectomics. nature methods **22**, 2463–2464 (2025)
4. Dorkenwald, S., Matsliah, A., Sterling, A.R., Schlegel, P., Yu, S.C., McKellar, C.E., Lin, A., Costa, M., Eichler, K., Yin, Y., et al.: Neuronal wiring diagram of an adult brain. Nature **634**(8032), 124–138 (2024)
5. Funke, J., Tschopp, F., Grisaitis, W., Sheridan, A., Singh, C., Saalfeld, S., Turaga, S.C.: Large scale image segmentation with structured loss based deep learning for connectome reconstruction. IEEE transactions on pattern analysis and machine intelligence **41**(7), 1669–1680 (2018)
6. Hildebrand, D.G.C., Cicconet, M., Torres, R.M., Choi, W., Quan, T.M., Moon, J., Wetzel, A.W., Scott Champion, A., Graham, B.J., Randlett, O., et al.: Whole-brain serial-section electron microscopy in larval zebrafish. Nature **545**(7654), 345–349 (2017)
7. Holler, S., Köstinger, G., Martin, K.A., Schuhknecht, G.F., Stratford, K.J.: Structure and function of a neocortical synapse. Nature **591**(7848), 111–116 (2021)
8. Huang, W., Deng, S., Chen, C., Fu, X., Xiong, Z.: Learning to model pixel-embedded affinity for homogeneous instance segmentation. In: Proceedings of the AAAI Conference on Artificial Intelligence. vol. 36, pp. 1007–1015 (2022)

9. Januszewski, M., Kornfeld, J., Li, P.H., Pope, A., Blakely, T., Lindsey, L., Maitin-Shepard, J., Tyka, M., Denk, W., Jain, V.: High-precision automated reconstruction of neurons with flood-filling networks. Nature methods **15**(8), 605–610 (2018)
10. Lee, K., Zung, J., Li, P., Jain, V., Seung, H.S.: Superhuman accuracy on the snemi3d connectomics challenge. arXiv preprint arXiv:1706.00120 (2017)
11. Liu, J., Yu, J., Shen, L., Chen, X., Ma, L., Zhai, H., Li, L., Zhang, L., Wang, L., Yuan, J., et al.: Connectomic organization of the suprachiasmatic nucleus. bioRxiv pp. 2024–10 (2024)
12. Matejek, B., Haehn, D., Zhu, H., Wei, D., Parag, T., Pfister, H.: Biologically-constrained graphs for global connectomics reconstruction. In: Proceedings of the IEEE/CVF conference on computer vision and pattern recognition. pp. 2089–2098 (2019)
13. Ngai, J.: Brain 2.0: Transforming neuroscience. Cell **185**(1), 4–8 (2022)
14. Qi, C.R., Su, H., Mo, K., Guibas, L.J.: Pointnet: Deep learning on point sets for 3d classification and segmentation. In: Proceedings of the IEEE conference on computer vision and pattern recognition. pp. 652–660 (2017)
15. Ravi, N., Gabeur, V., Hu, Y.T., Hu, R., Ryali, C., Ma, T., Khedr, H., Rädle, R., Rolland, C., Gustafson, L., Mintun, E., Pan, J., Alwala, K.V., Carion, N., Wu, C.Y., Girshick, R., Dollár, P., Feichtenhofer, C.: Sam 2: Segment anything in images and videos. arXiv preprint arXiv:2408.00714 (2024), `https://arxiv.org/abs/2408.00714`
16. Scheffer, L.K., Xu, C.S., Januszewski, M., Lu, Z., Takemura, S.y., Hayworth, K.J., Huang, G.B., Shinomiya, K., Maitlin-Shepard, J., Berg, S., et al.: A connectome and analysis of the adult drosophila central brain. elife **9**, e57443 (2020)
17. Schlegel, P., Yin, Y., Bates, A.S., Dorkenwald, S., Eichler, K., Brooks, P., Han, D.S., Gkantia, M., Dos Santos, M., Munnelly, E.J., et al.: Whole-brain annotation and multi-connectome cell typing of drosophila. Nature **634**(8032), 139–152 (2024)
18. Schmidt, M., Motta, A., Sievers, M., Helmstaedter, M.: Roboem: automated 3d flight tracing for synaptic-resolution connectomics. Nature methods **21**(5), 908–913 (2024)
19. Shapson-Coe, A., Januszewski, M., Berger, D.R., Pope, A., Wu, Y., Blakely, T., Schalek, R.L., Li, P.H., Wang, S., Maitin-Shepard, J., et al.: A petavoxel fragment of human cerebral cortex reconstructed at nanoscale resolution. Science **384**(6696), eadk4858 (2024)
20. Sheridan, A., Nguyen, T.M., Deb, D., Lee, W.C.A., Saalfeld, S., Turaga, S.C., Manor, U., Funke, J.: Local shape descriptors for neuron segmentation. Nature methods **20**(2), 295–303 (2023)
21. Turner, N.L., Macrina, T., Bae, J.A., Yang, R., Wilson, A.M., Schneider-Mizell, C., Lee, K., Lu, R., Wu, J., Bodor, A.L., et al.: Reconstruction of neocortex: Organelles, compartments, cells, circuits, and activity. Cell **185**(6), 1082–1100 (2022)
22. Zhang, Y., Guo, J., Zhai, H., Liu, J., Han, H.: Segneuron: 3d neuron instance segmentation in any em volume with a generalist model. In: International Conference on Medical Image Computing and Computer-Assisted Intervention. pp. 589–600. Springer (2024)